

# Reclaimed Laminate Waste as Novel, Heat Transfer Enhancing, Encapsulation for Long-term PCM Heat Storage

L. Desgrosseilliers<sup>\*,\*\*</sup>, D. Groulx<sup>\*\*,\*\*\*</sup> and M.A. White<sup>\*\*,\*\*\*\*</sup>

<sup>\*</sup>Mechanical Engineering, Dalhousie University, 5269 Morris Street, Room C360  
Halifax, NS, CAN, B3H 4R2, [louis.d@dal.ca](mailto:louis.d@dal.ca)

<sup>\*\*</sup>Institute for Research in Materials, Dalhousie University, Halifax, NS, CAN B3H 4R2

<sup>\*\*\*</sup>Mechanical Engineering, Dalhousie University, Halifax, NS, CAN, [dominic.groulx@dal.ca](mailto:dominic.groulx@dal.ca)

<sup>\*\*\*\*</sup>Chemistry, Dalhousie University, Halifax, NS, CAN, [mary.anne.white@dal.ca](mailto:mary.anne.white@dal.ca)

## ABSTRACT

Experimental evidence showed heat transfer improvements in laminated films made from polyethylene outer layers and an aluminum core. The mechanism for the heat transfer enhancements apply only to heat sources that do not cover the entire laminate sheet domain, i.e. finite heat sources. Seeded salt hydrate PCMs, used for seasonal heat storage, and ceramic stovetop heating elements are examples of finite heat sources. Theoretical 1D, symmetric heat balance equations were solved to predict temperature distributions in the aluminum core of the laminate sheets as well as the overall rate of heat transfer. Simulations in COMSOL Multiphysics 4.2a proved that the 1D equations captured the heat transfer mechanism with equal accuracy to 2D symmetric finite element solutions. Model validation was achieved using IR thermography of laminate films that were heated from behind with electric heating strips. Waste laminate sheets from post-consumer Tetra Pak cartons were obtained in house and from Klabin's paper mill in Piracicaba, Brazil.

**Keywords:** seasonal heat storage, salt hydrates, laminate encapsulation, theoretical heat transfer, experimental heat transfer

## 1 INTRODUCTION

Packaging, or encapsulation, of heat storage materials is essential in every application, and differs in scale (macro, micro, and bulk) and in some of its functions. For instance, microencapsulation can be used to disperse a heat storage material in a carrier solid to obtain high surface area for improved heat transfer; macroencapsulation can be made into long tubes of polymer or metal, small spheres, or panels to be used in modular heat storage systems; bulk encapsulation includes all forms of tank storage for the simplest, yet robust designs. Design requirements for encapsulation must address mechanical durability and integrity (leak proof), good heat transfer characteristics, vapour impermeability, and chemical compatibility [1], amongst other demands.

Seeded phase change materials (PCMs) used for long term/seasonal heat storage require further design requirements for proper encapsulation. Seeding is the

method by which an external crystal is added to a metastable, supersaturated salt hydrate solution in order to nucleate and cause the bulk system to solidify. In the case of seeding, encapsulation also must reliably accommodate an external seed trigger, which can be integral (e.g. flexible disc in therapeutic heat packs) or imbedded (e.g. seed injection nozzle).

Metal encapsulation is generally incompatible with salt hydrate PCMs (except for some stainless steels) [1,2] and typical rigid plastics cannot easily accommodate a solidification trigger (imbedded triggers only). Macroencapsulation pouches made of flexible laminate materials, however, have shown promise. Although the design of laminate packaging has been driven by requirements for barriers to water, air, and light to prevent food spoilage and degradation of consumer electronics, such packaging is resistant to chemical wear from salt hydrate solutions and is flexible and lightweight. Flexible packaging could easily incorporate integral or imbedded triggers and withstand dimensional changes from phase change processes. Lightweight laminate encapsulation also minimizes parasitic heat losses due the heat capacity of the inactive encapsulation material.

Lane [1,3] reported promising characteristics for 0.18 mm thick laminated polyethylene/aluminium/polyester pouches as salt hydrate PCM encapsulation for heat exchange with air. Schultz and Furbo [4] used 0.113 mm thick (9 µm thick Al foil) laminated pouches for their seasonal heat storage experiments (using supercooled NaCOOH·3H<sub>2</sub>O). Lane neglected any enhancements from the laminated film since the heat transfer medium, air, was the limiting factor, and the PCMs under study were only of the conventional, non-seeded kind, while Schultz and Furbo made their selection based on flexibility and shelf stability alone.

The true benefit of using laminate pouches is still largely unexplored. The stacked arrangement of dissimilar materials to which multi-ply cookware owes its heat transfer enhancements is a structure shared with laminate pouches, wherein the outside layers are made of tough, low thermal conductivity material, and the core layers are composed of high thermal conductivity metals.

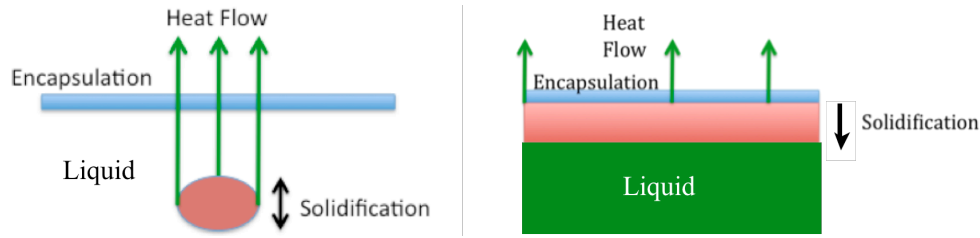


Figure 1: (left) Point heat source in seeded PCM; (right) solidification of a conventional PCM

## 2 HEAT TRANSFER MODEL

The mechanism for heat exchange during discharge of salt hydrate PCMs for long-term heat storage differs from conventional PCMs for short-term heat storage: seeding generates a finite heat source that grows from within the solution towards the container walls then expands along the length of the container, rather than a front that only expands inward from the walls (Fig. 1).

Finite heat sources present a challenge for conventional encapsulation, but the high thermal conductivity Al foil core in laminate pouches has the capacity to convey heat parallel to its surface, expanding the area for heat transfer. The latter can increase the overall rate of heat transfer. The theoretical and numerical heat transfer models under study capture what is a two-region fin model (Fig. 2).

The shape of the temperature profiles resulting from constant temperature heat sources depends only on the laminate's composition and dimensions as well as the length of the heat source ( $x, r = 0$  is the heat transfer axis of symmetry), while the magnitude depends only on the two temperature boundary conditions. The same applies to profiles resulting from constant heat flux finite heat sources, but the shapes of the profiles are markedly different (Fig. 3). For comparison, the equivalent temperature profile of a low-density polyethylene (LDPE) film numerically simulated in COMSOL Multiphysics 4.2a is also shown in Fig. 3.

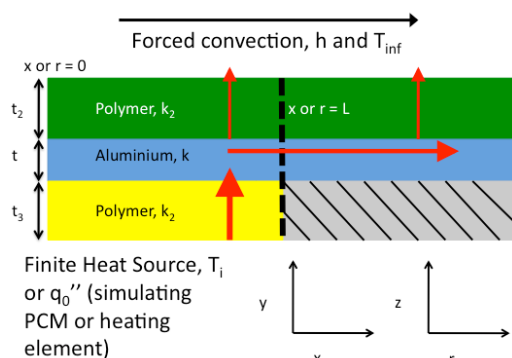


Figure 2: Two-region fin heat transfer model schematic.  $t$  represents thickness,  $x$  and  $r$  the respective axial position in cartesian and cylindrical coordinates,  $L$  the length of the applied heat source,  $h$  the convection coefficient,  $T_i$  and  $T_{inf}$  the applied temperature and free stream temperature, and  $q_0''$  the applied heat flux.

The predicted effectiveness of the modelled laminate heat transfer, meaning the ratio of laminate rate of heat transfer (two-region fin model) to that of a simple thermoplastic film, and the relative progression of the rate of fin heat transfer (unheated region), are shown in Fig. 4. Naturally, the effectiveness is  $\geq 1$ , but always decreasing with greater length of the heated domain.

## 3 EXPERIMENTAL VALIDATION

### 3.1 Materials and Method

Experiments were conducted for the constant heat flux boundary condition using flexible silicone rubber fiberglass insulated heaters from Omega (controlled by a STACO 0-140VAC VARIAC,  $\pm 0.5V$ ), while the remainder of the domain rested plainly on a sheet of 1" thick polystyrene foam insulation. The upper surface was allowed to exchange heat through natural convection.

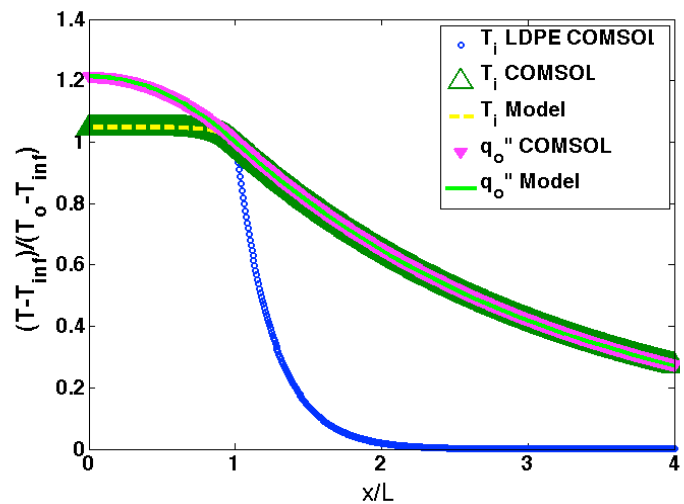


Figure 3: Dimensionless two-region fin model temperature profiles and others simulated in COMSOL.  $T_i$  and  $q_0''$  indicate solutions for applied temperature and applied heat flux boundary conditions in the heated domain,  $x \leq L$ .  $T_o$  is the  $x = L$  boundary temperature. All profiles, except the LDPE, overlap beyond  $x/L = 1$ .

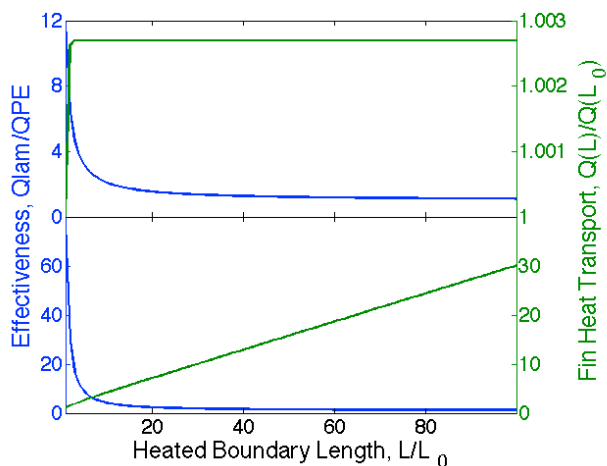


Figure 4: Laminate heat transfer effectiveness for constant temperature heat source only. Solution in rectangular coordinates (upper) and cylindrical coordinates (lower).  $L_o$  represents the smallest heated region in the solution set (1 mm); the fin heat transport is also relative to the solution at  $L_o$ .

T-type thermocouples adhered to the surface of the laminate (adhesive strips invisible to IR) recorded the surface temperatures in order to calibrate infrared thermographic images from an IR camera. Image intensities along cut lines were used to construct temperature profiles after calibration. Thermocouples on the surface of the laminate distorted local temperature fields (adding thermal resistance greater than the film), so they were kept along the outer edges of the film. Figure 5 shows the arrangement of thermocouples and their impact on the local temperature field. Experimental validation was performed for rectangular heat sources of heated lengths ( $L$ ) 2.54, 5.08, and 7.26 cm and rated power density of  $0.39 \text{ W cm}^{-2}$ .

The laminate films under examination were all sourced from used aseptic cartons, in this case 1 and 2 L Tetra Brik, which were separated from the outer paperboard and polyethylene layers by water immersion and light agitation/rubbing at room temperature for 35 min. This process mimics high consistency hydropulping done in paper mills to recycle the paperboard from cartons. Other

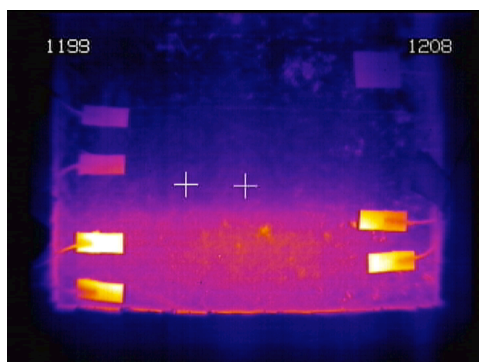


Figure 5: IR thermography showing thermocouples on Tetra Pak laminate film using a 5.08 cm heater.

samples were obtained from the high consistency hydropulper at Klabin's paper mill in Piracicaba, Brazil.

Aseptic cartons are already collected and sorted throughout the world (20% recycling rate worldwide in 2010 and 38% in Canada, 2011 [5,6]) with annual raw material consumption exceeding 0.75 Mt [7]. While the laminate in aseptic cartons only accounts for 26% [6] of the mass on average, it accounts for 55-59% of the embodied energy. The laminate films measured 100  $\mu\text{m}$  thick, with the layers measuring 32  $\mu\text{m}$  LDPE, 21  $\mu\text{m}$  Al, and 47  $\mu\text{m}$  thick.

The thermal conductivity of the laminate films measured at 30°C in a Mathis Instruments TC30 was  $0.42 \text{ W m}^{-1} \text{ K}^{-1}$ ; the thermal conductivity of polyethylenes (used in films) is between 0.33 and  $0.46 \text{ W m}^{-1} \text{ K}^{-1}$  [8] while that of Al is  $260 \text{ W m}^{-1} \text{ K}^{-1}$  [9].

### 3.2 Results and Discussion

The temperature profiles measured from IR thermography for the Al foil of the laminate pouches (LDPE is invisible to IR), with heaters operated at  $0.059 \text{ W cm}^{-2}$ , are shown in Fig. 6. Predictions from the proposed 1D symmetric, two-region fin model are also shown in Fig. 6 for the same experimental conditions.

The model predictions were obtained by adjusting the value of the heat transfer coefficient,  $h$ , in both the heated and unheated regions, separately, in a least-squares method of best fit. Although  $h$  is not predicted itself, it varies in the system due to the local intensity of natural convection, whereas the model assumes  $h$  is uniform over each region and makes no attempt to determine  $h$  from equations. Obtaining  $h$  by best fit still satisfies the energy balance and avoids further error from convection correlations, providing a better evaluation of temperature only. Since the samples were mounted vertically, with the heat source on the bottom, natural convection favoured the lowest regions, while promoting higher temperatures in the farther reaches of the heated region (as can be seen in Fig. 6) and imposing low convective cooling in the unheated region.

The temperatures measurements in the heated regions in Fig. 6 were subject to uncertainties between 1.2 and 2.5°C (except with the 2.54 cm heater, with 0.5 to 1.2°C everywhere), while IR calibration improved at the cooler temperatures of the unheated region, within 0.5 to 1.2°C. Error propagation from the two-region fin model, due to position, heat flux and temperature uncertainties, was between 0.51 and 0.60°C. Therefore, predicted temperature profiles matched closely with those from IR measurements and predictions were contained well within the measured temperature profile uncertainties. As a result, overall validation of the rectangular coordinates two-region model was achieved with medium to high accuracy.

Validation for constant heat flux was deemed sufficient to claim good predictive strength of the constant temperature finite heat sources (change in boundary condition only), relating to the objective of seeded PCM

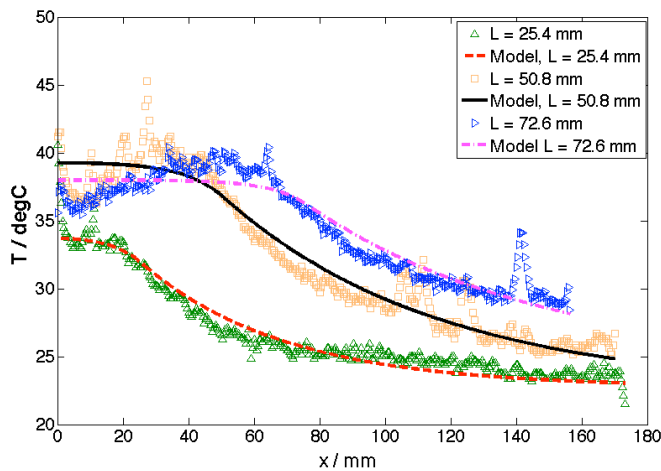


Figure 6: Experimental validation of the proposed two-region fin model in rectangular coordinates using two adjustable heat transfer coefficients to achieve best fit.

encapsulation. The temperature profiles in the heated region with applied  $T_i$  are simpler than with applied  $q_o''$ . The most important features of the temperature profile for the model to predict are the slope at the inflection point ( $x = L$ , edge of the heated boundary) and the temperature decay in the unheated region (fin region), observed in Fig. 6.

Good agreement of the model with experiment allows for a broader description of the range of performances that could be obtained for seeded PCMs. Figure 7 shows the domain range representing pouches  $8 \mu\text{m}$  to  $500 \mu\text{m}$  thick with a forced convection boundary condition equal to  $25 \text{ W m}^{-2} \text{ K}^{-1}$ ; with this information, a designer could optimize the heat transfer effectiveness for a given seeded PCM application.

## 4 CONCLUSION

With the achievement of medium to high accuracy validation for the proposed two-region fin model in cartesian coordinates (rectangular heat source) from this study, design calculations for heat transfer enhancements using laminate films to encapsulate salt hydrate PCMs can now be performed. As an additional benefit, the correct heat

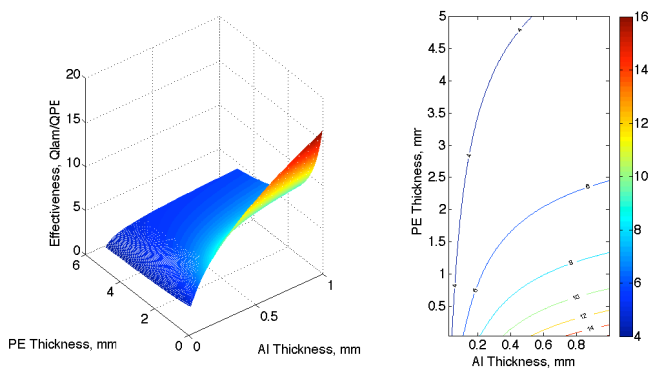


Figure 7: Domain map of heat transfer effectiveness solved for rectangular heat sources with applied  $T_i$  heat source.

dispersion performance of multi-ply cookware can also be described with the model equations, which could not be done before.

Rectangular heat sources are not the most common in nature, however they represent the lower bound of the observed behaviour, while circular heat sources (cylindrical coordinates solution) represent the upper bound. Thus, real systems fall between these geometries, with roundness being a desirable quality. The two-region fin model solution in cylindrical coordinates will soon follow with a separate validation.

## 5 ACKNOWLEDGEMENTS

The authors graciously acknowledge financial contributions from the Natural Sciences and Engineering Research Council of Canada (NSERC), Resource Recovery Fund Board (RRFB) of Nova Scotia, Dalhousie Research in Energy, Advanced Materials and Sustainability (DREAMS), and the Canada Foundation for Innovation (CFI). Technical expertise and use of equipment was assisted by the Institute for Research in Materials (IRM) at Dalhousie University, Klabin, Tetra Pak Brazil, EET Brasil (member of TSL Ambiental), Mokhtar Mohamed at Dalhousie University, and members of the Mary Anne White lab and the Lab of Applied MultiPhase Thermal Engineering (LAMTE).

## REFERENCES

- [1] G.A. Lane, "PCM Science and Technology: The Essential Connection," *ASHRAE Transactions*, vol. 91, 1897-1909, 1985.
- [2] D.H.B. Myron, *et al.*, "Computational Fluid Dynamics Modelling of Latent Heat Discharge in a Macro-Encapsulated Phase Change Material Device," in *7th International Energy Conversion Engineering Conference*, Denver, CO, 2009.
- [3] G.A. Lane, *et al.*, Report ORO/5217-8, Dow Chemical Company, Midland, MI, 1978.
- [4] J.M. Schultz and S. Furbo, "Storage Based on Phase Change Materials (PCM) Selection of Concepts," International Energy Agency February, 2005.
- [5] "Mission Possible: Sustainability Update 2011," Tetra Pak, Lund, Sweden, 2011.
- [6] Carton Council of Canada, Accessed April 11, 2012. <http://www.recyclecartons.ca/>.
- [7] Tetra Pak. Accessed November 29, 2011. <http://campaign.tetrapak.com/su2011/environment/naturalresources/seeing-the-wood-for.html#>.
- [8] E.H. Smith, "Mechanical Engineer's Reference Book," 12th ed., Elsevier, 1998.
- [9] J.R. Welty, *et al.*, "Fundamentals of Momentum, Heat, and Mass Transfer," 4<sup>th</sup> ed., Wiley: NY, 2001.